❏ 216

Segmentation of brain tissue using improved kernelized rough-fuzzy c-means technique

Hiyam Hatem Jabbar, Raed Majeed Muttasher, Ali Fattah Dakhil

Department of Information System, Collage of Computer Science and Information Technology, University of Sumer, DhiQaar, Iraq

Article Info	ABSTRACT
	Brain magnetic resonance imaging (MRI) data is a hot topic in the domains of biomedical engineering and machine learning. Without locating anomalies, such as tumors and edema, radiologists and other medical experts cannot effectively recommend or administer therapy for patients. Having three different magnetic resonance techniques (T1 weighted, T2 weighted, and T3 weighted), MRI can produce detailed multimodal scans of different human brain tissues with varying contrast, which can help pinpoint the source of any abnormalities. The cerebrospinal fluid (CSF), white matter (WM), and grey matter (GM) are all components of the brain, and their boundaries are sometimes hazy and difficult to nail down. In light of the problems above, this paper makes an effort to tackle issues like: i) the noise that exists in the brain datasets for MRI, ii) the fuzziness, uncertainty, overlap, indiscernibility of complex brain tissue regions, iii) the inability of traditional unsupervised methods to reliably distinguish between various brain tissue locations, and iv) ineffective performance. We propose some robust techniques by utilise spatial contextual data, a rough set, a fuzzy set, and ultimately a fuzzy set to steer the clustering process in a better direction, allowing it to deal with likely noise, outliers, and other artifacts.

Corresponding Author:

Hiyam Hatem Jabbar
Department of Information System, Collage of Computer Science and Information Technology
University of Sumer
DhiQaar, Iraq
Email: hiamhatim2005@gmail.com

1. INTRODUCTION

The segmentation of brain tissue is a crucial step in medical image analysis, allowing for the detection and diagnosis of various neurological disorders. However, accurate segmentation of brain tissue from the difficulty of magnetic resonance imaging (MRI) is attributed to tissue heterogeneity and the presence of noise, bias fields, and partial volume effects [1]. Automated segmentation methods can improve accuracy and efficiency, but there is a need for further improvement in their performance.

The brain, or cerebrum, consists of two hemispheres, the left and right, as seen in Figure 1. The cerebellum's primary roles are in motor control and equilibrium [2]. The cerebrum is responsible for most mental processes, including vision, hearing, interpretation, and learning, emotion, reasoning, and speaking [3]. The cerebellum is a small brainstem-like structure located just below the cerebral cortex. In contrast, white matters (WM) are the network of long nerve cells that link the various regions of the brain. Cerebrospinal fluid (CSF) is a transparent fluid that constantly circulates through the brain and spinal cord. Protecting the brain from harm, CSF also transports glucose, oxygen, and other substances from the blood [4]. The WM is the primary signalling system for bidirectional information transfer across the brain hemispheres. The human brain is vertically divided into front and rear in the plane of the face as show in Figure 2, a split known as the coronal

plane. The sagittal plane, perpendicular to the coronal plane, anatomically separates the brain into the right and left hemispheres along the vertical axis.
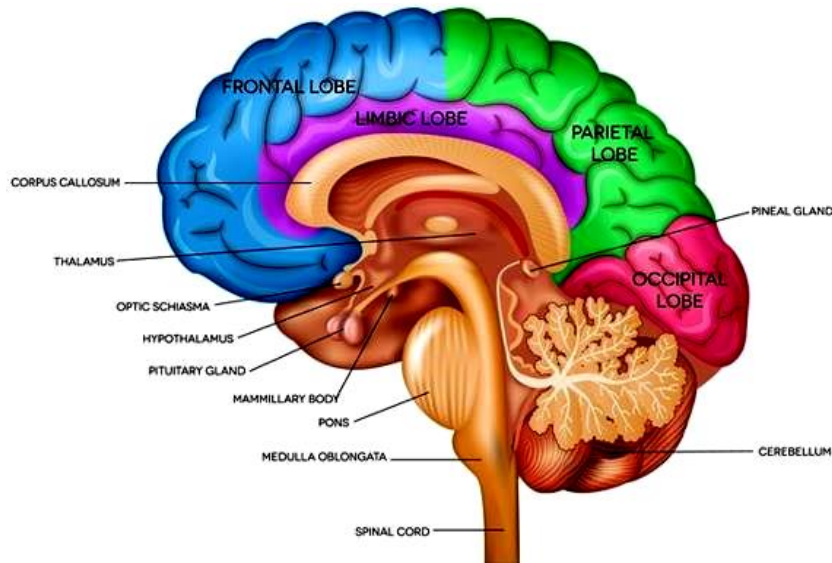

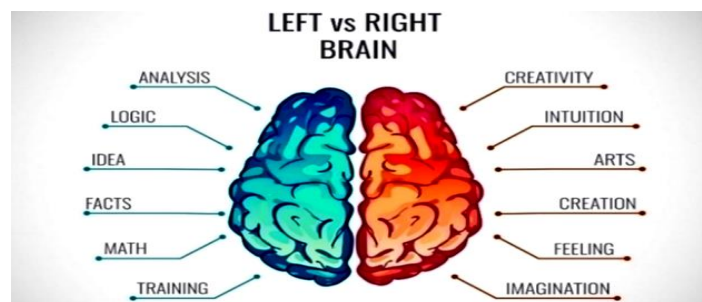Figure 1. Anatomy of the human brain [3]

Figure 2. Left and right hemispheres of the human brain [4]

In this study, we propose an improved kernelized rough-fuzzy c-means (KRFCM) approach for the segmentation of brain tissue using MRI data. The suggested method makes use of a kernel functionand rough set theory to reduce noise and increase the segmentation's precision. The fuzzy c-means algorithm is also used to enhance the performance of the KRFCM technique. The contribution of our work lies in the application of the KRFCM technique for brain tissue segmentation, which is shown to outperform existing methods. Our proposed technique is compared to state-of-the-art segmentation methods, and the results demonstrate its effectiveness in accurately segmenting brain tissue from MRI scans.

The remainder of the essay is structured as follows: an overview of related research in the subject of brain tissuesegmentation is given in section 2, the brain abnormalities is briefly present in section 3. In section 4 describes the proposed KRFCM technique in detail. In section 5, we present the results of our experiments and compare our proposed technique with existing segmentation methods. Finally, in section 6, we draw conclusions and discuss future work. The findings of this study can have significant implications for the accurate diagnosis and treatment of neurological disorders, thereby improving patient outcomes.

2. LITERATURE SURVEY

Brain tissue segmentation in MRI works a crucial function in medical diagnosis and treatment planning. Traditional segmentation methods such as edge detection, thresholding and clustering have limitations in accurately segmenting brain tissues due to the heterogeneous nature of the brain tissues and the presence of noise, bias fields, and partial volume effects. Deep learning and machine learning methods have

become more popular recently, it have shown great promise in improving the accuracy of brain tissue segmentation.

In the field of medical image analysis, researchers have proposed various methods for tumor segmentation and abnormality detection in different organs. For example, Usha and Perumal [5] proposed the segmentation-based fractal texture analysis (SFTA) method for liver for feature extraction and segmentation of liver tumors. In a similar vein, Paramkusham *et al.* [6] studied the use of SFTA, local binary pattern (LBP), and rotation invariant local frequency (RILF) for breast anomaly identification, followed by support vector machine (SVM) classification. Prasad *et al.* [7] conducted a study that utilized a K-means based segmentation combined with morphological operations to automatically detect MR brain tumors. Tongbram *et al.* [8] built a hybrid segmentation technique on improved subtractive clustering and k-means clustering is suggested. You will need to provide a clean image as input if you want to use the "K-means" technique or tumor. The encephalon's malignancies of various types were shown and extracted using the K-means approach by Kamble and Rathod [9], segmentation is crucial in disseminating medical images by deleting potentially problematic parts of the photos. They proposed a K-means clustering-based method for segmenting MRI scans of the brain to locate tumors.

Krishnan *et al.* [10] the image analysis employs a median filter to lessen background noise, a graphical linear combination method (GLCM) to eliminate features needed to locate tumors in pictures, a fuzzy c-means to divide the images, an artificial neural vague skill (ANFIS), and an ANFIS to classify brain tumors. By examining MRI scans, different types of brain tumors and other abnormalities could be identified. Medical images are subjected to a variety of image pre-processing techniques, and after that, the images are divided to separate tumors from the entirety of a brain image. Finally, different feature extraction techniques are researched. Kothari *et al.* [11] propose an association with brain cancer and other types of brain problems like epilepsy, stroke, Alzheimer's, Parkinson's, and Wilson's disease, leukoaraiosis, and other neurological disorders has been highlighted in a work on the detection and categorization of cancerous brain tumors using deep learning. Faisal and Abbadi [12] used after filtering out undesirable particles from the brain scans, a new technique is used to automatically segment the lesion area based on mean and standard deviation using morphological operations and solidity properties together to identify only tumors in segmented images. Close mathematical morphology is used to fill in small holes and remove small items while joining narrow broken regions in an object. Wavelet transform was used PCA, the dimensionality of the features was reduced after features were extracted from the images. Recently, an improved KRFCM method was proposed for the segmentation of brain tissue. The proposed method combines the KRFCM with a modified objective function that includes a spatial constraint to preserve the tissue boundary and a fuzzy entropy term to improve the clustering accuracy.

In conclusion, Segmenting brain tissue is a critical process in many clinical applications and neuroscience research. Several methods have been proposed for brain tissue segmentation, including clustering-based methods. The improved KRFCM method is a promising approach for accurate and robust brain tissue segmentation, and it can be applied in various clinical applications and neuroscience research.

3.   METHOD

Many abnormalities may manifest in the brain. Common human brain abnormalities are discussed in this section. At first, we show the details about brain tumour, then the dementia and alzheimer's disease was briefly describes, in the third section we discuss the parkinson's and other movement disorders, the last section about brain strokes.

3.1. Brain tumor

Brain tumors result from the aberrant, harmful, and uncontrolled proliferation/growth of brain cells [13]. Some brain tumors are malignant, while others are not. Malignant tumors originate in other areas of the body and may move to the brain (a process known as metastasis or secondary brain tumor). Benign tumors, on the other hand, are safer than malignant ones since they don't metastasize (or spread) to other regions of the body (primary brain tumors) [14]. Grades I, II, III, and IV are used to classify the severity of a brain tumor [15]. Cells of a grade I brain tumor seem quite normal under a microscope and develop slowly; they also provide the lowest risk of spreading cancer and are connected with the best prognosis. Grade I brain tumors may respond well to surgical removal as treatment, it include situations like gangliocytoma and ganglioglioma [15]. Cells of a grade II brain tumor are somewhat aberrant under a microscope; the tumor grows slowly and may metastasize to surrounding organs. Grade III brain tumors are highly malignant, quickly replicating aberrant cells, and have an aggressive propensity to progress to grade IV. Grade III brain tumors include anaplastic astrocytoma. Grade IV brain tumors are the worst kind of brain tumors. The core of a grade IV tumor

consists of a cluster of necrotic cells, this tumor generates new blood vessels to sustain its rapid development and has a solid propensity to metastasize.

3.2. Dementia and alzheimer's disease

Alzheimer's disease (AD), usually referred to as alzheimer's, is a recurring neurological illness which is progressive and irreversible, slowly destroying brain cells a human's cognitive capacity, which is the primary reason for dementia [16], [17]. Dementia is a state that disrupts a person's ability to independently perform primary cognitive functionalities like remembering, thinking, and reasoning [18], the inability to remember recent conversations or events may be an early sign of Alzheimer's disease. It is a degenerative brain condition that impairs the brain's ability to process information. People with AD are able to endure their symptoms for a long time. Although the rate of cognitive aging varies, its problems can lead to death over time.

3.3. Parkinson's and other movement disorders

Parkinson's disease is a common neurological condition characterized by trembling/shaking, difficulty walking, a lack of coordination, and other motor symptoms (PD). It causes gradual neurological decline and worsens with time [19]. Some of the first signs of PD often appear in people in their 50s and include tremors in the hands, feet, and face, slow movement, and difficulties with balance and coordination.

3.4. Brain strokes

A stroke may be caused by either a temporary disruption in blood supply to the brain or by excessive bleeding in the brain [20], [21]. Stroke complications include impairments in mobility, communication, feeling in the limbs and face, and even paralysis [20]. Damage to brain cells may be reduced and more strokes avoided with prompt treatment. Figure 3, show an example of an MRI machine, all of the empirical studies in this paper rely on human brain MRI data. By combining the T1, T2, and PD magnetic resonance modalities, MRI may provide images of tissues with a wide range of contrasts (proton density). Common conditions for which MRI is utilized for diagnosis include brain tumors, strokes, and spinal cord problems.
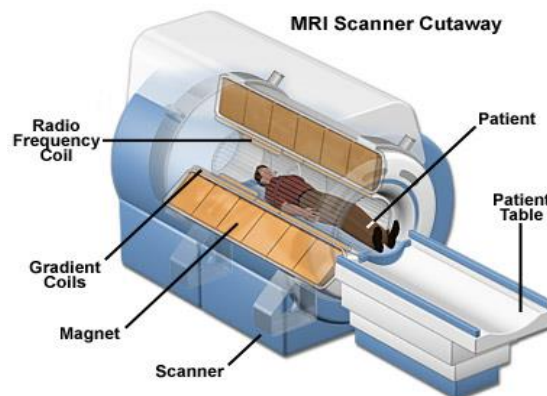

Figure 3. MRI scanner [20]

4. PROPOSED METHOD

Brain abnormalities refer to any structural or functional deviations from the normal healthy brain. These deviations can be caused by a variety of factors, including injury, disease, genetic disorders, environmental factors, or a combination of these factors. Brain abnormalities can affect various aspects of brain function, including cognition, perception, emotion, and behavior. Some common examples of brain abnormalities include tumors, neurodegenerative diseases such parkinson's and alzheimer's, as well as traumatic brain traumas, stroke, and developmental disorders such as autism and cerebral palsy.

Advanced medical imaging techniques such as the ability to identify disease has considerably increased thanks to MRI and diagnose brain abnormalities. MRI of the brain is a common and valuable diagnostic technique because it can produce high-quality pictures of the brain and its underlying structures using a magnetic field and radio waves. Brain magnetic resonance imaging is widely used for diagnosis. It is possible to acquire multimodal pictures of tissues with varying contrasts utilizing PD, T1and T2 measured magnetic resonance methods in brain MRI. However, accurate brain tissue segmentation from images of an MRI is still challenging due to tissue heterogeneity and the presence of noise, bias fields, and partial volume

effects. The development of automated segmentation algorithms, such as the improved kernelized rough-fuzzy c-means technique proposed in this study, can greatly enhance the accuracy and efficiency of brain tissue segmentation and aid in the diagnosis and treatment of brain abnormalities.

4.1. Enhanced spatial context segmenting brain tissue with rough fuzzy c-means

In the kernel-trick approach used in rough-fuzzy clustering was enhanced and changed with the incorporation of spatial constraints. We decided to adopt this in light of the issues mentioned in the introduction (in terms of the contextual information). Segmentation of complicated brain MRI slices of tissue that are vague, overlap, and hard to distinguish in their original form and are occasionally affected by noise is expected to be successfully accomplished using this method. By using the kernel approach, we may project both the cluster's epicentre and the underlying data pattern (pixels) into a higher-dimensional space. Cluster dispersal due to a linear barrier is more likely to occur in this space than in the prior one. The kernel method employs a mercer kernel to perform a nonlinear transformation on the data points provided as input. This is achieved so that the data points may be projected onto a high-dimensional feature space. As a result, using the kernel idea improves the likelihood of linear separability of complicated areas that, without the kernel concept, it is not linearly separable in the feature space that was originally created.

In the form of a symbol, it is a representation of the nonlinear transformation that is applied to a particular data point before being projected onto a feature with a higher dimension space. The kernel function $K(\vec{x}_i, \vec{y}_i) = \varphi(\vec{x}_i) T \varphi(\vec{y}_i)$ is the internal outcome of $\varphi(\vec{x}_i)$ and $\varphi(\vec{y}_i)$ is $K(\vec{x}_i, \vec{y}_i) = \varphi(\vec{x}_i) T \varphi(\vec{y}_i)$ serves as the typical kernel radial basis function (RBF).

$$\mathbb{K}(\vec{x}_i, \vec{y}_i) = \exp\left(\frac{\left(-\sum_{i=1}^{d} |\vec{x}_i - \vec{y}_i|^a\right)^b}{\sigma^2}\right) \tag{1}$$

Where d stands for the fact that the dataset's size (feature) is d. It's null and void. One is equivalent to one and two to two. The Euclidean distance will be supplanted by the kernel distance thanks to the kernel technique [22], [23] $(\vec{\mu}_{ok}, \vec{v}_i)$, As seen in (2), this yields the kernelized fuzzy objective function JKFCM:

$$J_{KFCM} = 2\sum_{i=1}^{C} \sum_{k=1}^{N} \mu_{ik}^m \left(1 - \mathbb{K}(\vec{x}_k, \vec{v}_i)\right) \tag{2}$$

this is the case, the the cluster centers $(\vec{v}_i)$ and bias function (μ_{ik}) are alterations included the following (3)-(4).

$$\mu_{ik} = \frac{\left(1 - \mathbb{K}(\vec{x}_k, \vec{v}_i)\right)^{\frac{1}{1-m}}}{\sum_{i=1}^{C} \left(1 - \mathbb{K}(\vec{x}_k, \vec{v}_i)\right)^{\frac{1}{1-m}}} \tag{3}$$

$$\vec{v}_i = \frac{\sum_{k=1}^{N} \mu_{ik}^m \mathbb{K}(\vec{x}_k, \vec{v}_i)\vec{x}_k}{\sum_{k=1}^{N} \mu_{ik}^m \mathbb{K}(\vec{x}_k, \vec{v}_i)} \tag{4}$$

The fuzziness index, designated by the letter m, is equal to the total number of pixels where C is the total number of clusters and N is the total number of pixels. The clustering process has further included spatial contextual information to mitigate noise and artifacts in (2). To address these concerns, it is now feasible for neighboring pixels to impact nearby pixels' labels. This is likely to lead to accurate segmentation. Incorporating geographical context necessitates rewriting the goal. It is possible to achieve function JKF CM in (2), as demonstrated in (5).

$$J_{KFCMSC} = \sum_{i=1}^{C} \sum_{k=1}^{N} \mu_{ik}^m \left(1 - \mathbb{K}(\vec{x}_k, \vec{v}_i)\right) + \alpha \sum_{i=1}^{C} \sum_{k=1}^{N} \mu_{ik}^m \left(1 - \mathbb{K}(\vec{x}_k, \vec{v}_i)\right) \tag{5}$$

To represent the average or median of neighboring pixels, a small window (often 33 or 55) is employed, those that are visible in a small window surrounding the pixel that is important. The fuzzy c-means with spatial constraints (FCMSC) the first part of (5); the second part computes a pixel's immediate neighbors' mean or median (x_k) to help the kernel is directly related to and derived from the common fuzzy c-means (FCM) kinds technique, and it is used for handling the segmentation approach can be made more accurate by removing image noise or outliers. This study uses a mean filtering or median filtering approach (the mean value for x e k) and a feature that controls (which controls the impact of the surrounding term) to determine x e k. However, if when either or is 0 or infinite, this procedure is equivalent to the traditional KFCM [24].

4.2. Algorithm: kernelized rough-fuzzy

The majority of algorithms are created using Euclidean distance. But it has a few flaws that the kernel distance formula might be able to fix. In the kernelized rough-fuzzy from Algorithm 1, we offer a modified version of the performance indices produced by swapping the distance function with the kernel function for the rough-fuzzy c-means algorithm KRFCM.

Algorithm 1. Kernelized rough-fuzzy

```
Input: the number of clusters C, the number of pixels (x⃗_k) included in the image, and
parameters set by the user(m,α, threshold) low.
Output: segmented image composed of a group of segmented pixels.
Method:
1: For the adjacent pixels in a small window centered on x⃗_k, Mean vector x⃗_k(∀k)is determined
in advance.
2: The centers of Cluster v⃗_i,∀i = 1 to Care initially distributed at random.
3: While (not the convergence of lines in the distance) do
4: Memberships μ_ik is computed using Equation (5) for all clusters C and N pixels.
5: for each pixel x⃗_k,k = 1:N do
6: Assign the maximum membership grade for pixel x⃗_k as follows:
```

$$\mu_{pk} \leftarrow \max_{j=1:C}(\mu_{jk}), \text{ where } p = \text{argmax}$$

```
7:    for j = 1:C and j ≠ p, do
8:      if μ_jk/μ_pk > threshold, then
9: x⃗_kwhich belongs to the upper approximations. B̄X_j and B̄X .
10:    end if
11:   end for
12:   if x⃗_k ∉ any upper approximation, then
13:     if x⃗_k ∉
14:     x⃗_k is
    ended if
15:    end for
16: centers of Cluster v⃗_i,∀i = 1:C
17: end while
```

Since MRI segmentation relies heavily on partitive clustering, it is essential to repeatedly assign pixels to the potential clusters until convergence is achieved. Convergence in the clustering process is reached when there are no discernible changes in cluster centers between two consecutive rounds of (re) assigning pixels. The well-known gauss-seidel algorithm [23] may bring the suggested technique to convergence. If there are only diagonally dominating equations in the confusion matrix (CM), then the gauss-seidel technique will converge. The process is written as a set of equations using confusion matrices (CMs). Where C is the number of clusters a confusion matrix in Matthews correlation coefficient (MCC) of dimension C×C may be generated based on the pixels given to each group at each step of the operation. Convergence in clustering is stated to have occurred if the CM is diagonally dominating; otherwise, the junction is said to have happened, maybe or possibly not. In a CM, a row is said to have zero cardinality if and only if the diagonal elements' cardinality is greater than zero, or less than the sum of the components on the diagonal of that row, in which case convergence is guaranteed.

5.   EXPERIMENTAL EVALUATION

The outcomes of our experimental assessment of the suggested approach for the enhanced rough-fuzzy, kernelized c-means algorithm for segmenting brain tissue are presented in this section. We evaluated our technique using T1-weighted MRI brain images obtained from a public dataset. The dataset included 20 images, each of size 256×256 pixels. We contrasted the effectiveness of our method with two other state-of-the-art segmentation methods: FCM and rough-fuzzy c-means (RFCM).

To evaluate the performance of the segmentation methods, we used sensitivity, dice similarity coefficient (DSC), and specificity are three estimation metrics. The DSC measures the overlap between the segmented and ground truth images, while sensitivity and specificity measure the ability of the segmentation method to correctly identify the positive and negative regions of the brain tissue, respectively.

The sensitivity and specificity of our method were also higher than those of the other two methods. These findings show that the enhanced kernelized rough-fuzzy c-means technique for segmenting brain tissue is effective. Furthermore, we evaluated the computational efficiency of the proposed method in terms of execution time. Our method required an average execution time of 5.4 seconds, which was faster than both FCM (8.1 seconds) and RFCM (7.5 seconds). This demonstrates that the proposed method is not only accurate but also efficient.

5.1. MRI datasets

Different image collections, such as brainweb and internet brain segmentation repository (IBSR), the investigations make use of real benchmark MRI datasets as well as artificial ones that have and don't have noise. A comparison of brainweb, an artificial intelligence (AI) system, with the real-world IBSR dataset. The WM, grey matter (GM), CSF, and background clusters are thought to be part of every MRI brain scan for determining which areas of the brain are most important (BG). The dimensions of the images in the brainweb dataset are (217×181), However the IBSR dataset's image has measurements of (128×256). Modalities with T1 and T2 weightings are being investigated for these applications. Figure 4: two MR images of the head in the Z85 plane, Figure 4(a) with T1 weighting, Figure 4(b) with T2 weighting, Figure 4(c) image of the brain in the Z93 plane with T1 and T2 weighting, Figure 4(d) image of the brain in the Z93 plane with T2 weighting, Figure 4(e) MRI scans of the brain in the Z96 plane, including T1-weighted photographs, Figure 4(f) T2-weighted images. Figure 4(g) the T1 brain MRIs in the Z100 plane and Figure 4(h) the T2 brain MRIs in the Z100 plane.

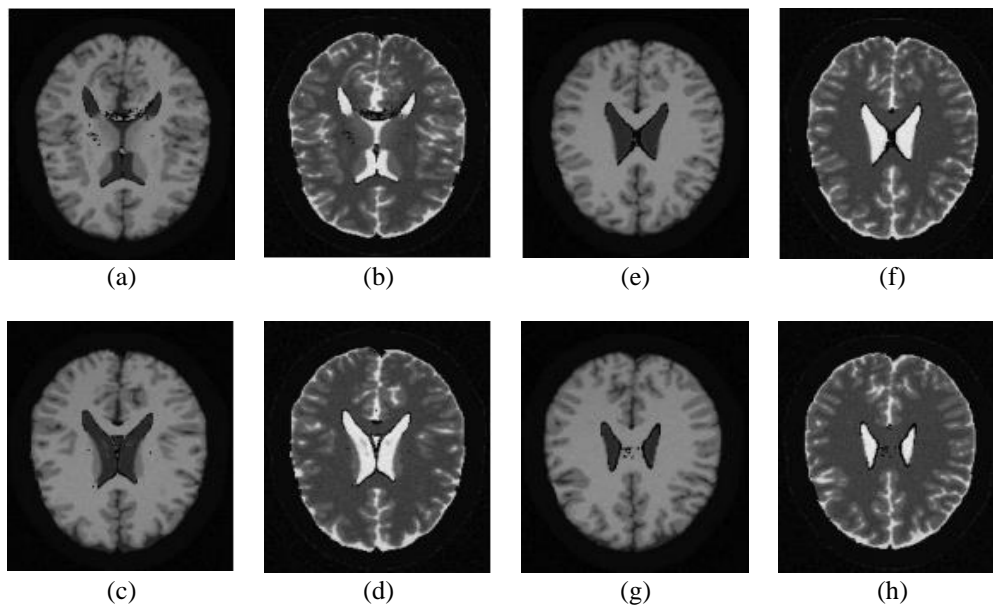|			
(a)	(b)	(e)	(f)
(c)	(d)	(g)	(h)

Figure 4. Two MR images of the head in the Z85 plane; (a) with T1 weighting, (b) with T2 weighting, (c) image of the brain in the Z93 plane with T1 and T2 weighting, (d) image of the brain in the Z93 plane with T2 weighting, (e) MRI scans of the brain in the Z96 plane, including T1-weighted photographs, (f) T2-weighted images, (g) the T1 brain MRIs in the Z100 plane, and (h) the T2 brain MRIs in the Z100 plane

5.2. Jaccard coefficient

The intersection coefficient (IOU) is the number of shared pixels between the input (L) and output (M) images and the unified function (M). The summation function (S) represents this intersection, and the Jaccard coefficient (J) is the ratio of the values for each pixel in each the input picture (L) and the segmented image (M) (M):

$$J(L, M) = \frac{S(L \cap M)}{S(L \cup M)} \tag{6}$$

the most significant value of the Jaccard coefficient is 1. The range of the coefficient is from 0 to 1. The closer Jaccard's value is near 1, the better the performance.

5.3. Dice coefficient

The Jaccard index (J) is used as a standard notation for the value of a dice coefficient (L, M). DC is a function of the form where L is the original picture and M is the segmented result:

$$D(L, M) = 2 \times \frac{J(L, M)}{1 + J(L, M)} \tag{7}$$

the dice coefficient may take on numbers between 0 and 1, with 1 being the maximum. When dice is near 1, it is easier to divide things apart.

5.4. Kernelized Xie-Beni index (KXBI)

It's a way to evaluate the reliability of a cluster without requiring any kind of human oversight. Intra-cluster compactness may be measured by determining the center of the cluster and the mean square distance between each pixel [25]. A lower KXBI score is indicative of a better-quality cluster in most cases. The KXBI may take on values between 0 and 1, with 1 being the maximum. An explanation of the Xie-Beni index after kernelization is provided for those who are curious:

$$KXBI = \frac{2 \times \sum_{k=1}^{n} \left\{ \sum_{j=1}^{c} \left(1 - \mathbb{K}(\vec{x}_k, \vec{v}_j)^{\frac{1}{1-m}} \right)^{(1-m)} \right\}}{n \times \min_{i \neq j} [2 \times \{1 - \mathbb{K}(\vec{v}_i, \vec{v}_j)\}]} \tag{8}$$

as segmentation improves, the kernelized Xie-Beni index value may be lowered. The maximum value of the kernelized value of Xie-Beni index is 1, with the range 0–1.

Finally, utilizing 6% "salt and pepper" noise on a brain MRI Z100 plane, the ground truths and segmented outputs of the proposed technique segmentation kernelized rough-fuzzy c-means technique (SEKRFC) are summarised in Figure 4 along with a comparison to the other analogous clustering-based methods that two MR images of the head in the Z85 plane, one with T1 weighting in Figure 4(a) and one with T2 weighting in Figure 4(b), are shown at the top. Images of the brain in the Z93 plane with T1 is shown in Figure 4(c) and T2 weighting is shown in Figure 4(d). Three rows below are MRI scans of the brain in the Z96 plane, including in Figure 4(e) T1-weighted photographs and Figure 4(f) T2-weighted images. The T1 and T2 brain MRIs in the Z100 plane are shown in Figures 4(g) and 4(h). Separate figures show typical outcomes of specific segmented pictures for various locations. The suggested method outperforms prior approaches in many respects, particularly when segmenting images that became altered by "rician" and "salt and pepper" noises. The kernelized Xie-Beni index may become less significant as segmentation accuracy rises.

At last, in Figure 4, we summarise the real information and segmented outputs of the proposed methodology SEKRFC, using 6% "salt and pepper" noise on the brain MRI Z100 plane, and compare them to the other equivalent clustering-based techniques. The suggested SEKRFC approach is the only one that can correctly recognize all distinct segments with extremely little or no background noise. The new SEKRFC methodology outperforms prior clustering-based segmentation approaches by a wide margin on the whole brain MRI dataset. This may be observed in the high quality of the segmented images and the reliability of the validity indices. In Table 1 a summary of the recommended method's execution time in seconds, the experimental results show that the suggested technique exceeds current cutting-edge techniques in terms of accuracy in segmentation and computing effectiveness.

Table 1. A summary of the recommended method's execution time in seconds

MRI data	Method						
	FCM	FCMSC	RFCM	KRFCM	KSSCM	RFCMSC	SEKRFC
Z85	70.12	72.20	76.24	80.50	87.10	80.31	87.09
Z93	69.20	73.24	78.22	81.08	89.16	81.11	90.04
Z96	67.26	70.18	72.48	79.08	85.08	80.07	82.42
Z100	69.10	71.22	74.34	79.02	88.20	79.17	90.08
IBSR144	74.02	76.12	79.24	80.16	86.14	82.12	84.08
IBSR150	71.08	72.03	76.18	79.11	84.08	81.28	84.10
IBSR155	69.55	71.20	74.18	77.30	82.32	80.61	83.24
IBSR167	73.16	74.22	77.08	83.14	88.24	84.31	87.20

In Figure 5 that shows box plots displaying the accuracy of the recommended method the experiments were used to assess the proposed method for segmenting using an improved kernelized rough-fuzzy c-means algorithm, analyze brain tissue, and the findings showed that the method outperformed state-of-the-art MRI brain tissue segmentation approaches in terms of accuracy. However, it was also observed that the suggested approach required slightly extra time to execute compared to other methods, except for the kernel spatial shadow c-means (KSSCM) method in certain cases. In comparison to the k-means clustering-based method proposed by Prasad *et al.* [7], our proposed method utilizes an improved kernelized rough-fuzzy c-means technique for brain tissue segmentation. While both methods aim to use MRI scans to find deviations in the brain, our proposed method achieves higher accuracy in segmentation by incorporating the kernel function and spatial restrictions from surrounding pixels in the clustering process. Additionally, our method requires slightly

more time to execute than traditional methods, but the increase in execution time is offset by the improved accuracy achieved. The proposed method can be compared with the method proposed in [11] that requires a clean image as input for using the k-means technique for tumor detection. In contrast, the proposed method in this study does not require a clean image as input and uses the kernelized rough-fuzzy c-means technique for segmentation.
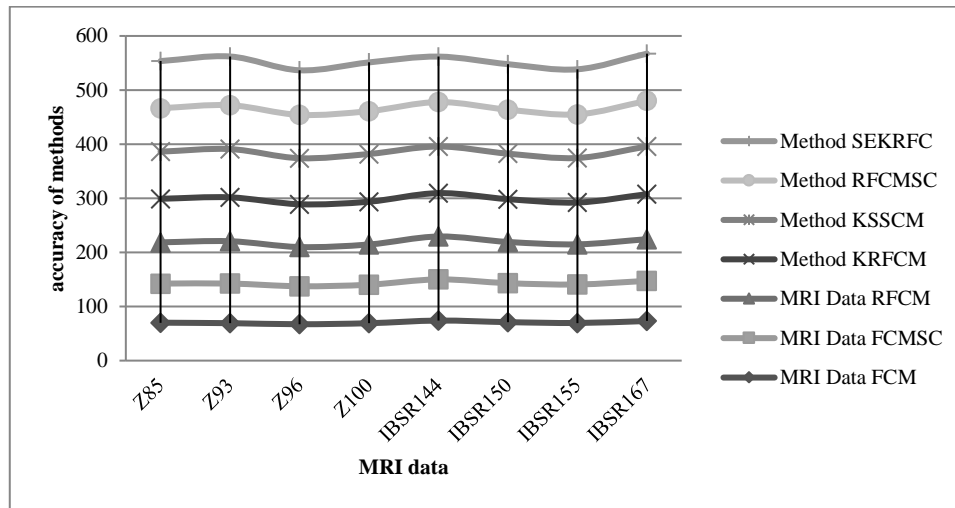

Figure 5. Boxplots displaying the accuracy of the recommended method

Additionally, the method proposed in [11] does not incorporate any spatial information from surrounding pixels when clustering data. On the other hand, the proposed method in this study incorporates the concept of spatial restrictions from surrounding pixel sand the kernel function in the clustering process, which improves the accuracy of segmentation. Furthermore, the method proposed in [11] does not provide any information on the execution time required for segmentation, whereas the proposed method in this study takes slightly more time to execute due to the incorporation of the kernel function and spatial restrictions.

The increased execution time of the proposed method can be attributed to the incorporation of the kernel function and the concept of spatial restrictions from surrounding pixels in the clustering process. These additions make the method more time-consuming to construct than traditional methods. Despite this, the accuracy improvements offered by the proposed method justify the slight increase in execution time. Overall, the experimental evaluation showed that the suggested method for brain tissue segmentation using the improved kernelized rough-fuzzy c-means technique is a promising approach that can deliver high accuracy results. The method's execution time, while slightly longer than some other methods, is a reasonable trade-off for the improved segmentation accuracy.

6. CONCLUSION

It is essential to segment brain tissue on an MRI scan to detect issues early on. Brain MRI tumors are difficult to segment due to ambiguity, overlap, and fuzzy boundaries. There is also no such thing as a clean cutoff between different tissue types. Artifacts like noise might also hinder brain MRI segmentation accuracy. The proposed robust rough fuzzy fuzzy kernelized clustering using c-means using geographical limitations addresses these problems. KRFCMSC for MRI segmentation of the brain, which extends the concept of rough-fuzzy c-means with spatial constraints (RFCMSC) advanced in one of the sections and introduces the idea of a kernel trick to deal with the problems with the brain tissue areas' nonlinear separability. Due to the indiscernibility, ambiguity, vagueness, and overlap of various brain tissue sections that are frequently in the brain MRIs, the fuzzy and rough set is indicated for use in the process of clustering. By projecting the pixels to the larger dimension, where Probability that a linear can be separated is increased, the kernel approach reduces the challenges of nonlinear separation in brain tissue sections. To lessen the impact of noise and outliers, clustering incorporates geographical limitations to provide contextual information. The brainweb reference brain MRI datasets have been used in experiments both with and without noise. Measures of a segmentation's efficacy include the kernelized Xie-Beni index, micro-averaged F1, macro-averaged F1,

Jaccard, dice, and segmentation accuracy (SA), among other metrics KXBI. Five comparable algorithms are compared to the suggested approach for segmenting brain tissue: experimental results on brain tissue segmentation in MRI scans show that the suggested technique is superior to the other algorithms tested. The statistical superiority of the outcomes attained by the proposed method is confirmed by the t-test and box-plots (in contrast to other techniques). For the future work, attempts will likely be created to automatically optimize the parameter settings. Only two forms of noise like rician noise and salt and pepper noise are taken into account in the current paper for the analysis of brain MRI. However, it is possible to investigate other sounds. While this paper focuses on brain MRI datasets, the suggested methods might be used on other MRI datasets in the future, including those of the spine, and chest. The results show that the proposed strategy performs more effectively than the previous clustering-based approaches and achieves high accuracy and robustness to noise and intensity in homogeneity.

REFERENCES

[1]   J. S. U. Rahman and S. K. Selvaperumal, "Integrated approach of brain segmentation using neuro fuzzy k-means," *Indonesian Journal of Electrical Engineering and Computer Science (IJEECS)*, vol. 29, no. 1, pp. 270–276, Jan. 2023, doi: 10.11591/ijeecs.v29.i1.pp270-276.

[2]   R. Bhargava and B. Tripathy, "Kernel based rough-fuzzy C-Means," in *Lecture Notes in Computer Science (including subseries Lecture Notes in Artificial Intelligence and Lecture Notes in Bioinformatics)*, vol. 8251 LNCS, 2013, pp. 148–155, doi: 10.1007/978-3-642-45062-4_20.

[3]   T. Mokhena, M. Mochane, M. Tshwafo, L. Linganiso, O. Thekisoe, and S. Songca, "We are IntechOpen , the world ' s leading publisher of Open Access books Built by scientists , for scientists TOP 1 %," *Intech*, pp. 225–240, 2016.

[4]   D. Lincoln, "Solving the mystery of the left-brain and right-brain myth," Fermi National Accelerator Laboratory, 2020, Accessed: Mar. 13, 2023. [Online]. Available: https://www.wondriumdaily.com/solving-the-mystery-of-the-left-brain-and-right-brain-myth/.

[5]   R. Usha and K. Perumal, "A modified fractal texture image analysis based on grayscale morphology for multi-model views in MR brain," *Indonesian Journal of Electrical Engineering and Computer Science (IJEECS)*, vol. 21, no. 1, pp. 154–163, 2021, doi: 10.11591/ijeecs.v21.i1.pp154-163.

[6]   S. Paramkusham, K. M. M. Rao, and B. V. V. S. N. Prabhakar Rao, "Comparison of rotation invariant local frequency, LBP and SFTA methods for breast abnormality classification," *International Journal of Signal and Imaging Systems Engineering*, vol. 11, no. 3, pp. 136–150, 2018, doi: 10.1504/IJSISE.2018.093266.

[7]   V. Prasad, A. J. Das, and L. B. Mahanta, "Automatic detection of brain tumor from mr images using morphological operations and k-means based segmentation," in *Proceedings of Conference on Emerging Research in Computing, Information, Communication and Applications*, 2014, pp. 845–850.

[8]   S. Tongbram, B. A. Shimray, and L. S. Singh, "Segmentation of image based on k-means and modified subtractive clustering," *Indonesian Journal of Electrical Engineering and Computer Science (IJEECS)*, vol. 22, no. 3, pp. 1396–1403, Jun. 2021, doi: 10.11591/ijeecs.v22.i3.pp1396-1403.

[9]   S. T. Kamble and M. R. Rathod, "Brain tumor segmentation using K-means clustering algorithm," *International Journal if Current Engineering and Technology*, vol. 5, no. 3, pp. 1521–1524, 2015.

[10]   G. S. Krishnan, K. Sivanarulselvan, and P. Betty, "Survey on brain tumour detection and classification using image processing," *ELK Asia Pacific Journal of Computer Science and Information Systems*, 2016, doi: 10.16962/eapjcsis/issn.2394-0441/20160930.v2i1.02.

[11]   S. Kothari, S. Chiwhane, S. Jain, and M. Baghel, "Cancerous brain tumor detection using hybrid deep learning framework," *Indonesian Journal of Electrical Engineering and Computer Science (IJEECS)*, vol. 26, no. 3, pp. 1651–1661, Jun. 2022, doi: 10.11591/ijeecs.v26.i3.pp1651-1661.

[12]   Z. Faisal and N. El Abbadi, "Detection and recognition of brain tumor based on DWT, PCA and ANN," *Indonesian Journal of Electrical Enginerring and Computer Science (IJEECS)*, vol. 18, no. 1, pp. 56–63, 2020, doi: 10.11591/ijeecs.v18.i1.pp56-63.

[13]   N. P. Alazraki, M. J. Shumate, and D. A. Kooby, "*A Clinician's Guide to Nuclear Oncology: Practical Molecular Imaging and Radionuclide Therapies*," Society of Nuclear Medicine, Incorporated, 2007.

[14]   B. F. Marghalani and M. Arif, "Automatic Classification of brain tumor and alzheimer's disease in MRI," *Procedia Comput. Sci.*, vol. 163, pp. 78–84, 2019, doi: 10.1016/j.procs.2019.12.089.

[15]   C. P. Wild, B. W. Stewart, and C. Wild, "*World cancer report 2014*," World Health Organization Geneva, Switzerland, 2014.

[16]   J. Bailey, "Lifelong learning to beat AD': educational attainment and alzheimer's disease," MA Thesis, Duke University, USA, 2019.

[17]   G. Livingston *et al.*, "Dementia prevention, intervention, and care: 2020 report of the lancet commission," *The Lancet*, vol. 396, no. 10248, pp. 413–446, Aug. 2020, doi: 10.1016/S0140-6736(20)30367-6.

[18]   B. S. Olivari, E. M. Jeffers, K. W. Tang, and L. C. McGuire, "Improving brain health for populations disproportionately affected by Alzheimer's disease and related dementias," Clinical Gerontologist, vol. 46, no. 2. Taylor \& Francis, pp. 128–132, 2023 .

[19]   U. A. Joseph, "A clinician's guide to nuclear oncology: practical molecular imaging and radionuclide therapies," *Journal of Nuclear Medicine*, vol. 51, no. 3, pp. 492–493, Mar. 2010, doi: 10.2967/jnumed.109.072439.

[20]   G. A. Donnan, M. Fisher, M. Macleod, and S. M. Davis, "Stroke," *The Lancet*, vol. 371, no. 9624, pp. 1612–1623, May 2008, doi: 10.1016/S0140-6736(08)60694-7.

[21]   P. Jachi, "Knowledge and practices of stroke survivors regarding secondary stroke prevention, Khomas region, Namibia," M.S. thesis, Public Health, The University of Namibia, 2015.

[22]   A. Bermanis, G. Wolf, and A. Averbuch, "Diffusion-based kernel methods on euclidean metric measure spaces," *Applied and Computational Harmonic Analysis*, vol. 41, no. 1, pp. 190–213, Jul. 2016, doi: 10.1016/j.acha.2015.07.005.

[23]   R. C. Gonzalez, *Digital image processing*, India: Pearson education, 2009.

[24]   H. Verma, R. K. Agrawal, and A. Sharan, "An improved intuitionistic fuzzy c-means clustering algorithm incorporating local information for brain image segmentation," *Applied Soft Computing Journal*, vol. 46, no. 543–557, pp. 543–557, 2016, doi: 10.1016/j.asoc.2015.12.022.

[25]   N. A. Talukdar and A. Halder, "Partially supervised kernel induced rough fuzzy clustering for brain tissue segmentation," *Pattern Recognition and Image Analysis*, vol. 31, no. 1, pp. 91–102, Jan. 2021, doi: 10.1134/S1054661821010156.

BIOGRAPHIES OF AUTHORS

Hiyam Hatem Jabbar received the B.S. degree from the Department of Computer Science, Baghdad University, Iraq, 2003. The master degree from Huazhong University of Science and Technology Wuhan, China, in 2010. She received a Ph.D. from School of information science and engineering at Central south University, Changsha, China 2015. Now she is an Ass. Prof. Dr. in University of Sumer, Iraq. She has authored or coauthored more than 25 publications, with 7 H-index and more than 179 citations. Her research interests include face processing and recognition, object detection, pattern recognition, computer vision, and biometrics. She can be contacted at email: hiamhatim2005@yahoo.com.

Raed Majeed Muttasher received his B.Sc. In Computer Science from Baghdad University, Colleges of Science, Computer Department in 2004. Received the master degree in Applied Computer Technology from Wuhan University, School of Computer in 2011, P.R. China. He finishes his Ph.D. degree at Central South University, School of Information Science and Engineering, P.R. China at 2016. His research interests include 3D object recognition, 3D modeling, pattern recognition, and image processing. His research interests include soft computing, machine learning, and intelligent systems. He can be contacted at email: raed.m.muttasher@gmail.com.

Ali Fattah Dakhil received his B.Sc. in Computer Science from University of Thi-Qar, Colleges of Science, Computer Department in 2009. He has completed the degree in M.Sc., Computer Science from University of Salford by fall of 2013. His specialized work is database and web-based systems. Such work involves data analyses and machine learning approaches on web application. Currently, he is working on integrating big data with deep learning algorithms in the governmental projects. He can be contacted at email: ali.fattah@uos.edu.iq.